Design of a New Dual-Frequency and Dual-Polarization Microstrip Element

Reuven Shavit, *Senior Member, IEEE,* Yuval Tzur, and Danny Spirtus, *Associate Member, IEEE*

***Abstract*—A new type of a dual-frequency and dual-linear-polarization multilayer stacked microstrip antenna element is presented. The feeding mechanism of the element is aperture coupling for one polarization and direct feeding for the orthogonal polarization. The microstrip element exhibits a wide band of operation, high isolation between ports, and high radiation efficiency for both polarizations compared to other type of elements. A parametric study was conducted using a commercial software based on method of moments (MoM) algorithm and is presented. A prototype with dimensions based on the simulations was built and tested. The agreement between the measured and numerical results is good.**

***Index Terms*—Dual frequency, dual-polarization, microstrip antenna, multilayer.**

I. Introduction

MICROSTRIP patch antenna elements are very popular in wireless communication system applications. They offer an attractive way to integrate the radio frequency (RF) front end of the system with the radiating antenna and achieve a low profile, low weight, easy fabrication, and low-cost solution. In the design of a dual-frequency and dual-polarization microstrip antenna, a few concerns are addressed: frequency bandwidth for both polarizations, isolation between ports, radiation efficiency, and feeding mechanism, which will guarantee minimum losses, minimum stray radiation, and avoid topology problems in an array application. A simple microstrip patch antenna element has a relatively narrow frequency bandwidth (less than 5%), which in most wide band applications is insufficient. Parasitic patches/dipoles on top or aside the driving patch/dipoles [1]–[4] are a possible solution to this deficiency. The parasitic patches/dipoles load reactively the driving patch/dipole in a way that widens the frequency bandwidth of the element. There are numerous ways to feed the microstrip patch, such as direct coaxial feeding [5] or direct microstrip feeding [6], aperture coupling to a microstrip line [7], aperture coupling to a stripline [8], and electromagnetic coupling [9]. A one-layer direct feeding for dual-polarization array application encounters feeding network topology difficulties. It is clear that the proper way to avoid this difficulty is to use a multilayer feeding network structure. In this case, the real challenge is to transfer the energy from layer to layer with minimal losses. The obvious possibility for the energy transfer among layers is to use vias (conductive pins). However, this mechanism is lossy, has low isolation between adjacent ports, and adds complexity to the fabrication process. Accordingly, aperture or electromagnetic coupling among layers seems to provide the correct solution.

In this paper, we present a new dual-frequency and dual-polarization microstrip element. Two stacked parasitic patches are used to independently control the frequency bandwidths of the two feeding ports of the microstrip element. The feeding element mechanism is based on aperture coupling for one polarization and direct feeding for the orthogonal polarization. This concept results in a multilayer structure with different dielectric constants. The computation of the radiation parameters and currents was conducted using the *IE3D* commercial software from *Zeland*, which is based on a MoM algorithm. A parametric study on the parasitic patch dimensions and the layers thickness was performed to obtain optimum performance of the return loss (two polarizations), maximum radiation efficiency, and the maximum isolation between the input ports. A prototype of the element in the Ku band was built and tested. The agreement between the computed and the test results is good.

II. Analysis

Fig. 1 shows the basic structure of the proposed element. The driven rectangular patch dimensions are L_{1x} and L_{1y}, in which L_{1x} stands for the resonant length in x direction (port 1) and L_{1y} for the resonant length in y direction (port 2). The patch is printed on a dielectric layer with thickness H_1, dielectric constant ε_{r1}, and loss tangent $tan\delta 1$. The patch is driven directly by a microstrip line at port #1 and is aperture coupled at port #2. The two orthogonal feeding mechanisms at the two ports generate radiation in two polarizations and in two frequency bandwidths. The dimensions L_{1x} and L_{1y} control the central frequencies of each frequency band. A slot in the ground plane with dimensions *SL* (slot length) and *SW* (slot width) is driving the patch at port #2. The slot is electromagnetically excited by a stripline embedded in a dielectric layer with thickness H_f, dielectric constant ε_{rf}, and loss tangent $tan\delta_f$. Unfortunately, the stripline structure supports, in addition to the desired stripline transverse electromagnetic (TEM) mode, an additional parallel plate TEM mode. The generation of the parallel plate mode may be detrimental to the feeding network losses, therefore its excitation has to be avoided. This mode is excited near stripline discontinuities and in the slot close proximity. A possible way to suppress the generation of the parallel plate TEM mode is to insert metallic vias on both sides of the slot [10]. These vias

Manuscript received January 10, 2002; revised May 31, 2002. This work was supported by Gilat Satellite Networks Ltd., as part of Gilat's new generation of VSAT products.

R. Shavit is with Department of Electrical and Computer Engineering, Ben-Gurion University of the Negev, Beer Sheva 84105, Israel.

Y. Tzur was with Gilat Satellite Networks Ltd., Petah Tikva 49130, Israel. He is now with M.T.I Wireless Edge, Rosh Ha'ayin 48091, Israel.

D. Spirtus is with Gilat Satellite Networks Ltd., Petah Tikva 49130, Israel.

Digital Object Identifier 10.1109/TAP.2003.813594

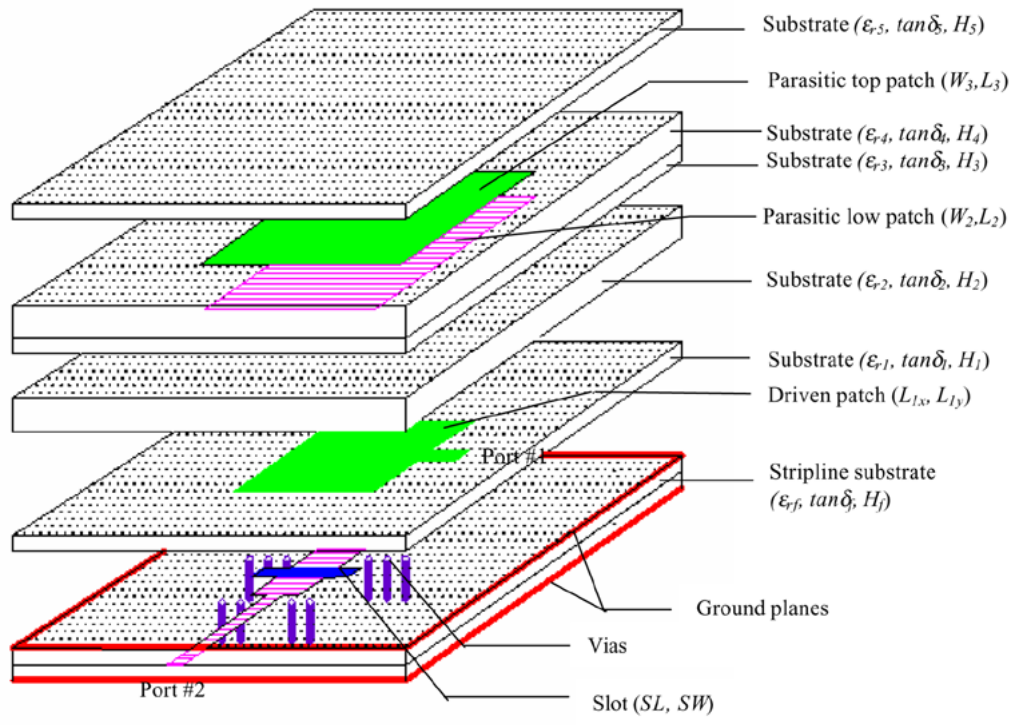

Fig. 1. Geometry of the dual-frequency, dual-polarization microstrip antenna.

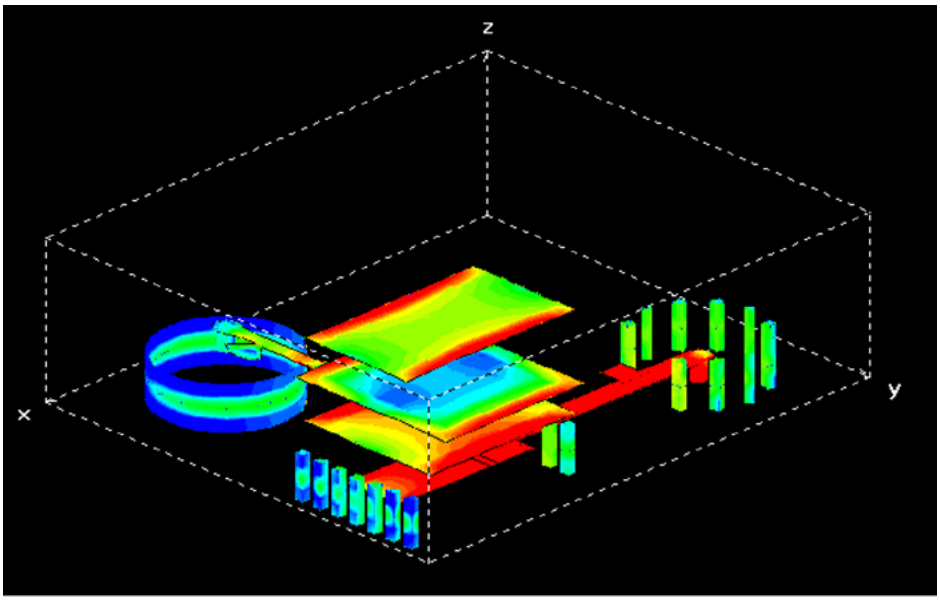

Fig. 2. Current distribution at 11.2 GHz with port #2 excited.

suppress the parallel plate mode, but allow propagation of the stripline TEM mode.

The use of stacked parasitic patches to increase the frequency bandwidth of a single polarization microstrip element is well documented in [11] for direct feeding, in [1] for aperture-coupled feeding, and in [3] for electromagnetic coupling. However, it turns out that the optimum substrate geometry for the aperture coupled feeding mechanism is different from that for the direct feeding mechanism. Accordingly, one parasitic patch cannot accommodate optimum performance for both feeding mechanisms. The solution is to use two parasitic patches at different levels above the driven patch and control independently the two frequency bands. The lower parasitic patch dimensions are (W_2, L_2) and is separated from the driven patch by a dielectric layer with thickness H_2 and electrical properties (ε_{r2}, $tan\delta_2$). The top parasitic patch dimensions are (W_3, L_3) and is separated by two dielectric layers with thickness H_3 and H_4, with electrical properties (ε_{r3}, $tan\delta_3$) and (ε_{r4}, $tan\delta_4$), respectively. The top dielectric substrate with thickness H_5 and electrical properties (ε_{r5}, $tan\delta_5$) are only for protection purposes.

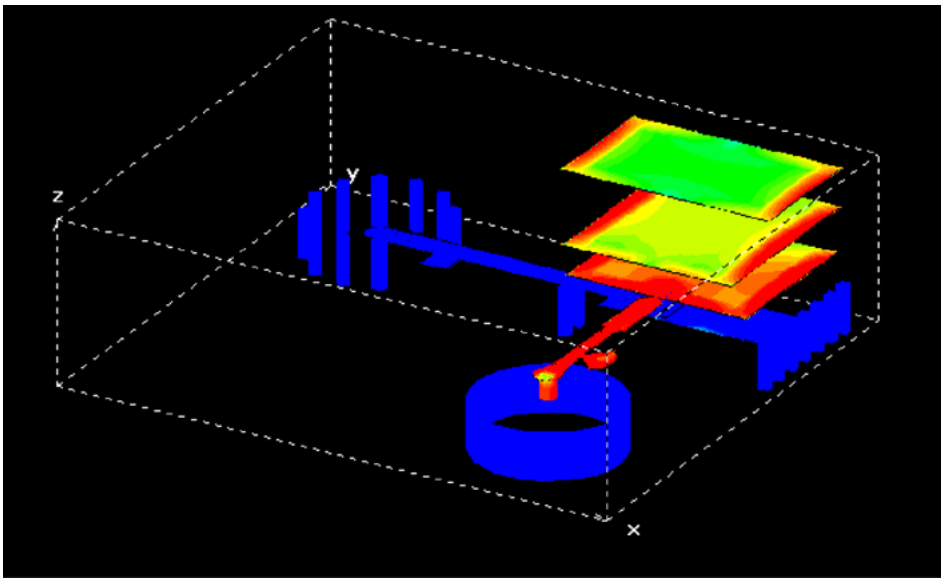

Fig. 3. Current distribution at 14.25 GHz with port #1 excited.

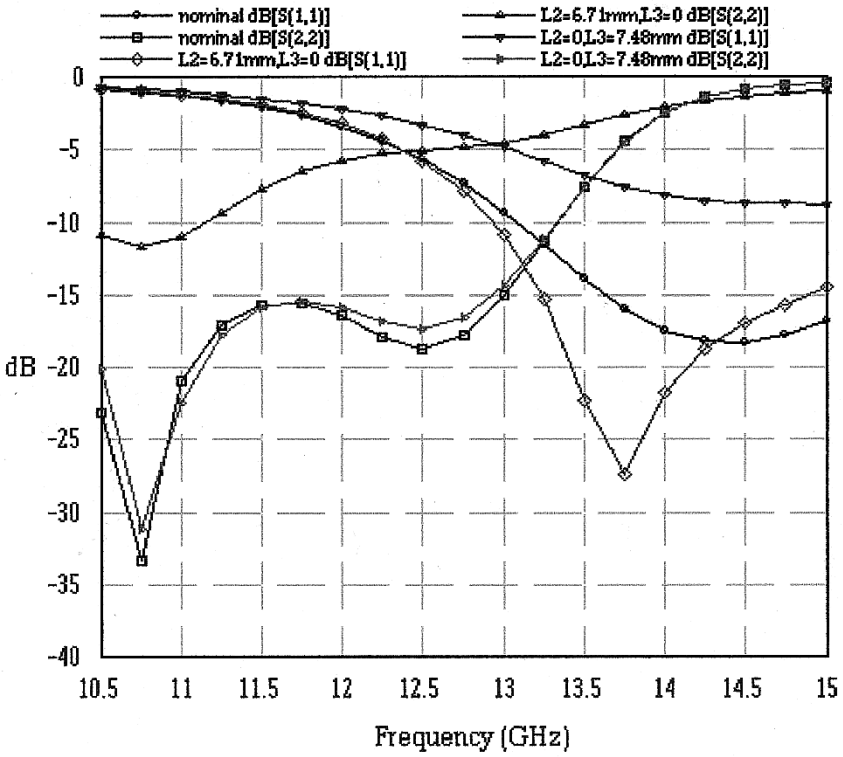

Fig. 4. Return loss at port #1 and #2 with and without the top and bottom parasitic patches.

The element was designed to operate between 10.9–12.7 GHz at port #2 and 14–14.5 GHz at port #1. To reduce the fabrication cost of the element, low-cost materials were considered. Thus, the stripline substrate chosen was RO4003 from Rogers with $H_f = 1.62$ mm and electrical properties $\varepsilon_{rf} = 3.38$, $tan\delta_f = 0.002$. The driven patch was printed on MX-243 from Metclad with $H_1 = 0.762$ mm and electrical properties $\varepsilon_{r1} = 2.43$, $tan\delta_1 = 0.002$. The substrate above the driven patch is foam with $H_2 = 1.2$ mm and electrical properties $\varepsilon_{r2} = 1.067$, $tan\delta_2 = 0.0041$. The low parasitic patch is printed on a thin substrate of MX-280 from Metclad with $H_3 = 0.05$ mm and electrical properties $\varepsilon_{r1} = 2.88$, $tan\delta_1 = 0.008$. The top parasitic patch is separated from the low parasitic patch by a foam substrate with $H_4 = 1.8$ mm and electrical properties $\varepsilon_{r4} = 1.067$, $tan\delta_4 = 0.0041$. The top layer is RO4003 with $H_5 = 0.2$ mm and electrical properties $\varepsilon_{r5} = 3.38$, $tan\delta_5 = 0.002$. The slot dimensions were chosen to be $SL = 5.04$ mm, $SW = 0.35$ mm. The driven patch dimensions were $L_{1x} = 6.42$ mm and $L_{1y} = 5.63$ mm. The dimensions of the lower parasitic patch were $L_2 = 6.71$ mm, $W_2 = 6.08$ mm and those of the top parasitic patch were $L_3 = 7.48$ mm, $W_3 = 4.49$ mm. The vias diameter is 0.3 mm and theirs center to center spacing is 0.8 mm.

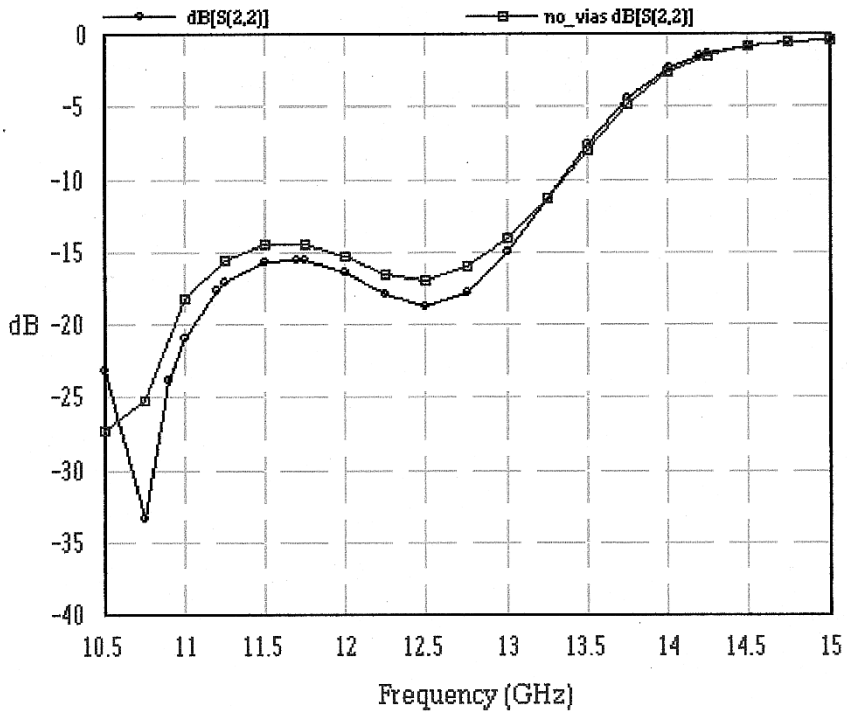

Fig. 5. Return loss at port #2 with and without the conductive vias on both sides of the slot.

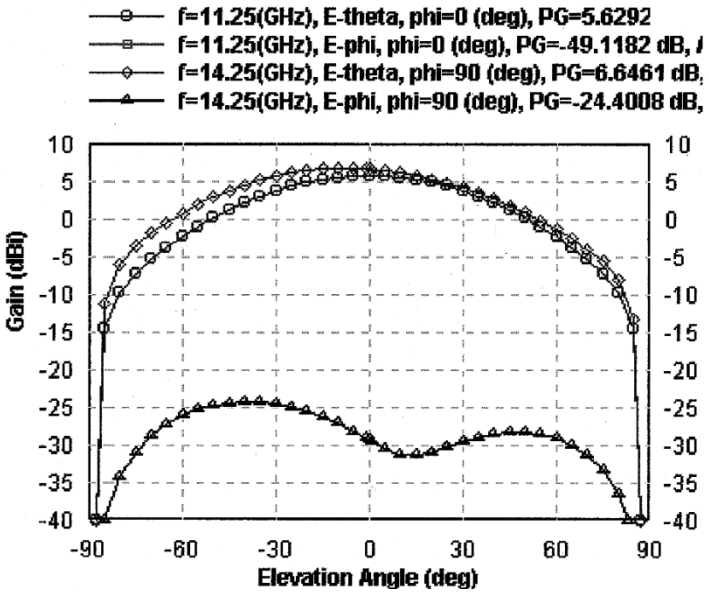

Fig. 6. Copol (E_θ) and Xpol (E_ϕ) element radiation patterns at 11.25 and 14.25 GHz.

To obtain matching to a 50-Ω impedance level at both ports, $\lambda/4$ microstrip transformers and parallel stubs were used. The length of the $\lambda/4$ transformer at port #1 is 2.6 mm and its width is 0.8 mm, while at port #2 the length is 3 mm and the width is 2.36 mm. The matching stubs used on both ports are based on 50-Ω characteristics impedance microstrip and stripline with dimensions: width of 0.52 and 0.92 mm, and length of 1.25 and 0.81 mm, respectively. The distance between ports was 14.2 mm.

The performance of the element was computed using the *IE3D* software from *Zeland.* The software is based on MoM+algorithm optimized for multilayer structures. Figs. 2 and 3 show the current distribution at 11.2 and 14.25 GHz on the driven and the parasitic patches for excitation at ports #2 and #1, respectively. One can observe that at 11.2 GHz, only the driven and top parasitic patches are excited, while at 14.25 GHz, only the driven and low parasitic patches are excited, emphasizing the orthogonal effect of the low and top parasitic patches on the two polarizations and dual-frequency bands. This behavior is also emphasized in Fig. 4, which displays the return loss at both ports with and without the top or low parasitic patches compared to the element with both parasitic patches. Again, one can observe the deterioration in performance on the low- and high-frequency bands in the absence of the top or bottom parasitic patches. Fig. 5 shows the effect of the conductive vias

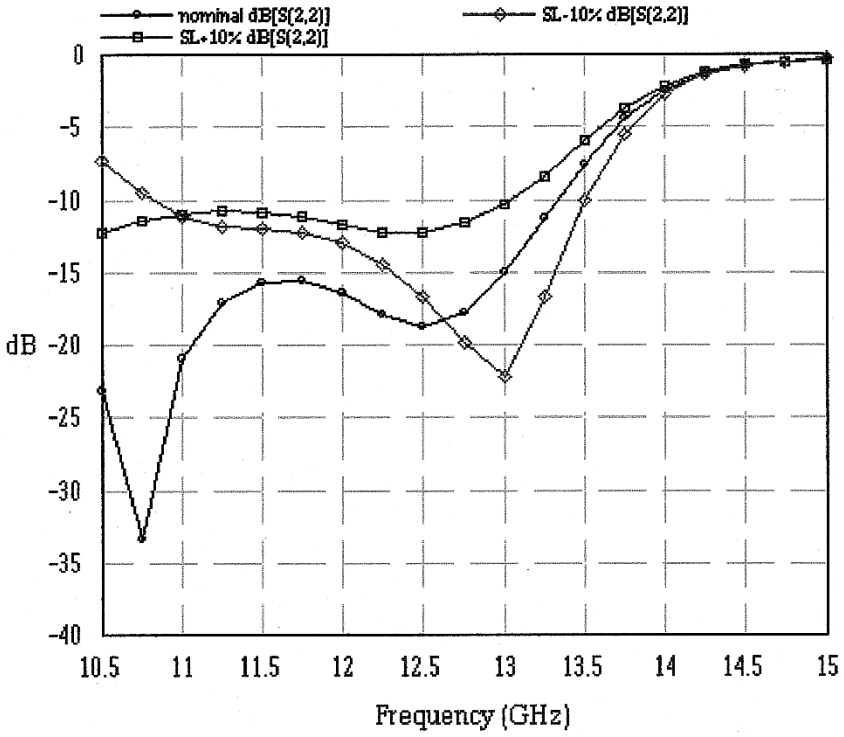

Fig. 7. The effect of the coupling slot length variation ($\pm 10\%$) on the return loss at port #2.

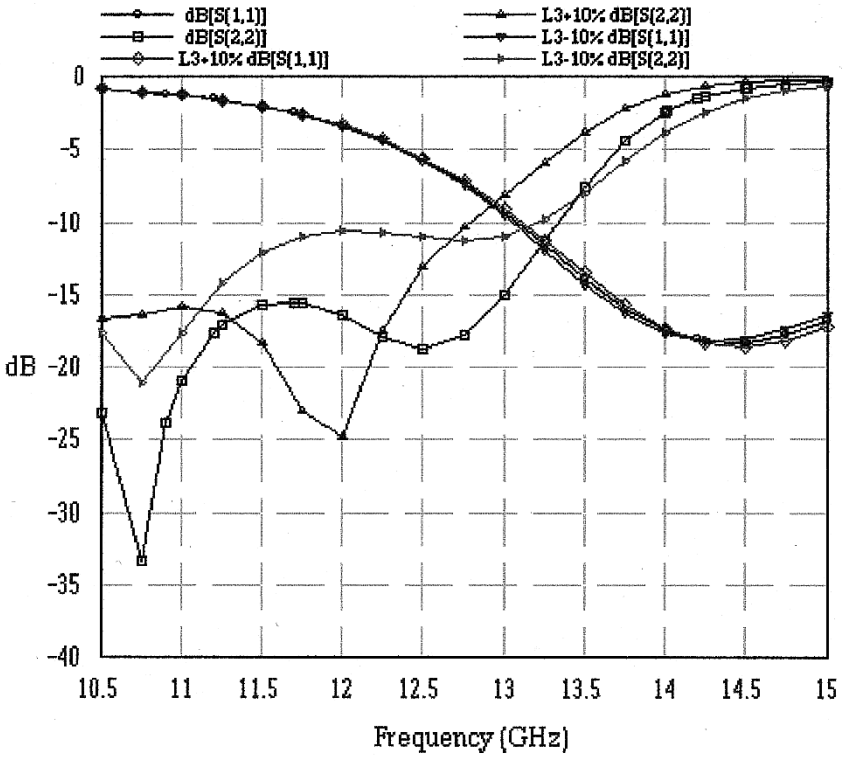

Fig. 8. Effect on the return loss at both ports with the top parasitic patch length, L_3 variation.

on the return loss at port #2. One can notice deterioration in performance without their existence, which is a clear indication of the parallel plate mode excitation. The radiation characteristics of the radiating element are shown in Fig. 6. One can observe almost no variation in the Copol (E_θ) radiation patterns at the center frequencies 11.25 and 14.25 GHz of the two ports. However, significant difference can be noticed in the Xpol (E_ϕ) levels at the two ports. The Xpol level on the boresight axis at port #2 at 11.25 GHz is -49 dB, while the Xpol level at port #1 is -30 dB. This difference can be attributed to the fact that

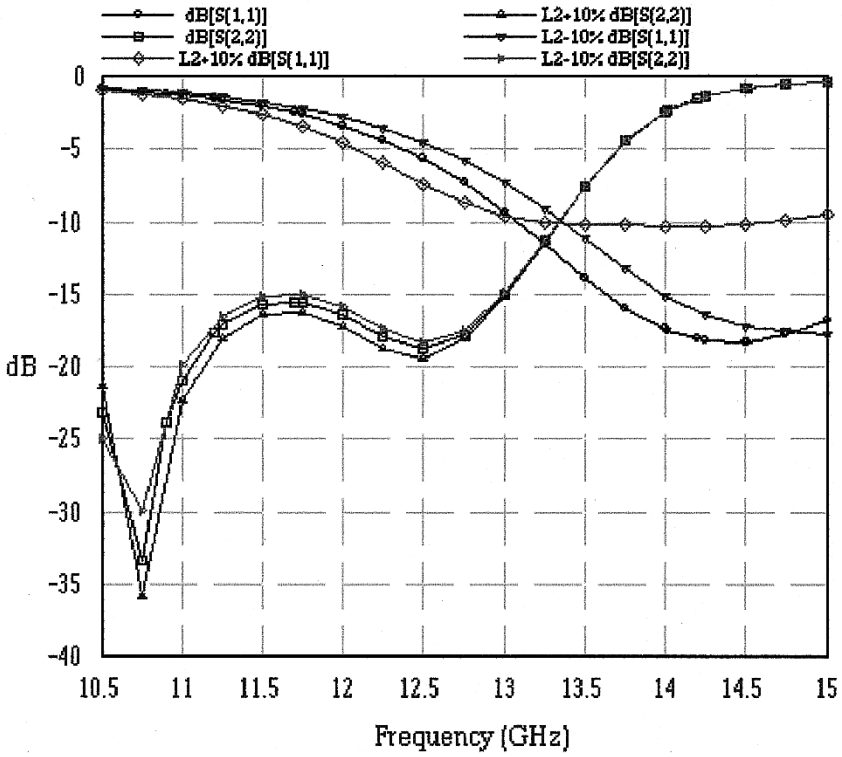

Fig. 9. The effect on the return loss at both ports with the bottom parasitic patch length, L_2 variation.

the feeding line at port #2 is shielded (stripline) and no feeding line radiation exists. In this case the Xpol level is determined solely by the radiating element, which is very low. At port #1 the Xpol radiation is dominated by the radiation from the microstrip feeding line and, accordingly, its level is higher.

III. Parametric Study

In this section, we will consider the sensitivity of the device parameters to changes in the element dimensions. Fig. 7 shows the effect on the return loss due to the coupling slot length variation ($\pm 10\%$). One can observe that the center frequency increases or decreases in proportion to the slot length and total bandwidth narrows in both cases. Fig. 8 shows the effect on the return loss at both ports for the top parasitic patch length, L_3 variation. It is interesting to note that this variation has almost no effect on the performance at port #1, which reinforces the assumption of orthogonal effect of the two parasitic patches on the two frequency bands. An increase or decrease in the center frequency proportional to the parasitic patch length, L_3 can be noticed. Fig. 9 shows the effect on the return loss at port #1 for the bottom parasitic patch length, L_2 variation. The effect is similar to that shown in Fig. 8, with ports #1 and #2 interchanged. It can be noticed that variation of L_2 has a minimal impact on the performance at port #2 (lower frequency band). Figs. 10 and 11 show the effect on the return loss on both ports for variation of the foam thickness layers H_4 and H_2, respectively. As expected, the effect of the top layer thickness H_4 variation is more significant in the low frequency band (port #2), while it has a minimal effect on the upper frequency band (port #1). In analogy, variation of H_2, affects the performance at port #1 and has a minimal effect at port #2.

A prototype of the element was built and tested. The multilayer substrate dimensions were 5×5 cm. Fig. 12 shows the comparison of the measured and computed results of the return loss frequency dependence at both ports and the isolation between the two ports. One can observe a better agreement of the computed and measured return loss results at port #1. The trend of the measured and computed return loss results at port #2 is good even though the absolute values are not in good agreement. The possible reason for the disagreement is insufficient suppression of the parallel plate mode, which is reflected from the edges of the prototype. This phenomenon cannot be identified in the computation, which assumes infinite substrate layers and as such avoids reflections from the edges. The measured and computed results of the isolation S_{21} is in good agreement and shows isolation better than 60 dB in the upper frequency band and better than 45 dB in the lower frequency band. Comparison simulations conducted with the same device but coaxially fed on both ports result in isolation of only 25 dB in the lower frequency band and 35 dB in the upper frequency band. A parametric study of the distance between the feeding ports proved that the isolation between ports is almost independent on the distance between the feeding ports due to the physical separation of the stripline feeding port from the direct feeding port. In case of direct feeding for both polarizations (ports), the isolation is highly dependent on the distance between ports, since they coexist on the same substrate. These results prove the advantage of the proposed feeding technique (aperture coupling combined with direct feeding) compared to the direct feeding (coaxial or microstrip). Fig. 13 shows the frequency dependence of the measured and computed gain of the element at both ports. The maximum gain obtained at both ports is 7.5–8 dBi. As can

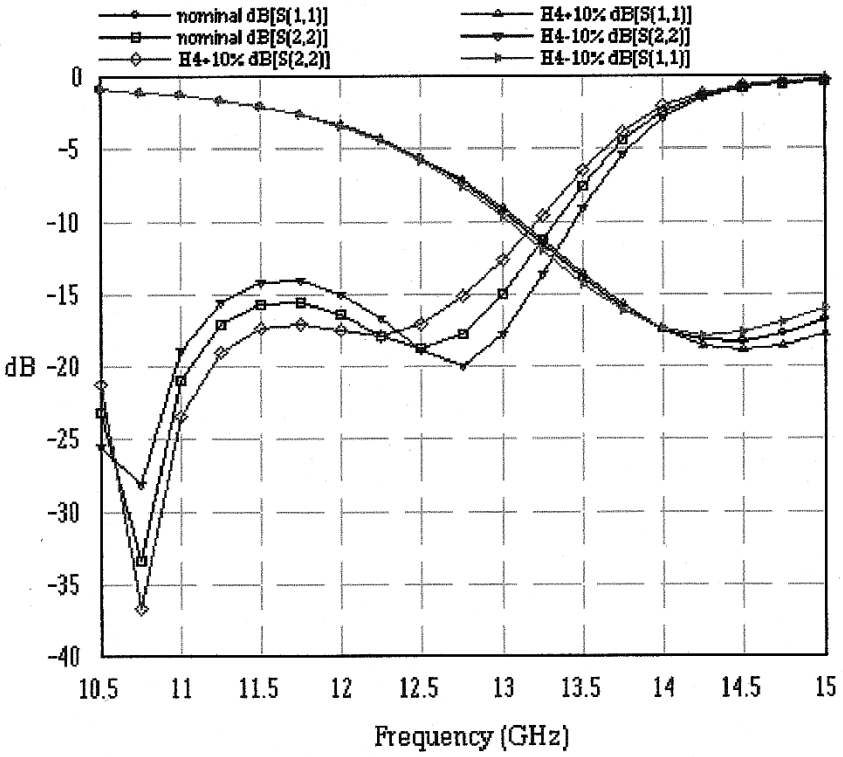

Fig. 10. Return loss at port #1 and #2 with variation of the foam thickness layer H_4.

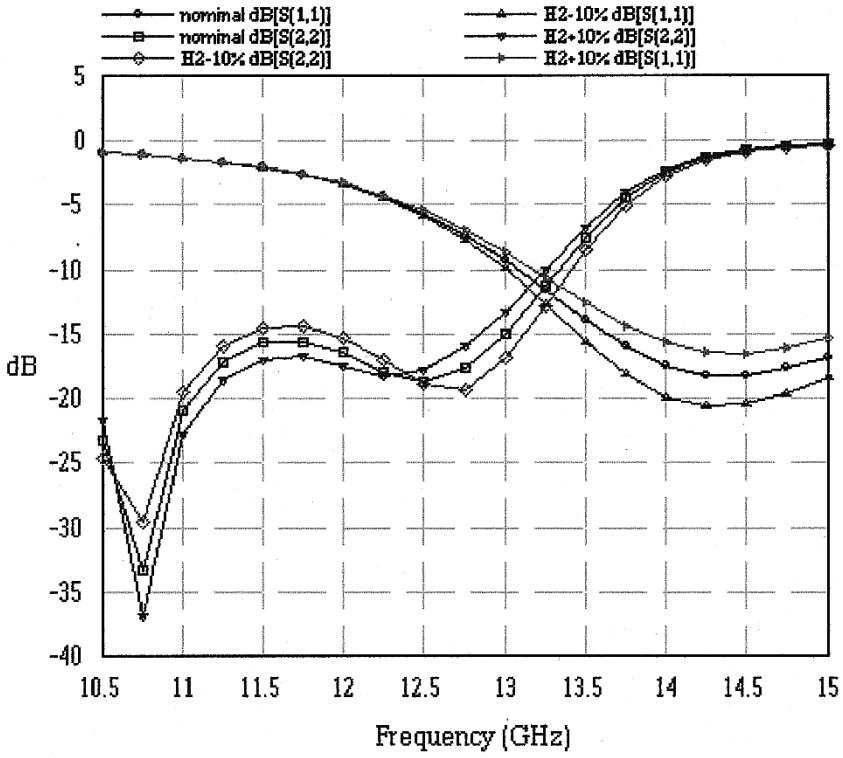

Fig. 11. Return loss at port #1 and #2 with variation of the foam thickness layer H_2.

be noticed, the agreement between the computed and measured results is better at port #1. The disagreement at port #2 may be caused from the same reasons mentioned previously: insufficient suppression of the parasitic parallel plate mode and diffraction from the prototype edges, which adds additional losses to the system.

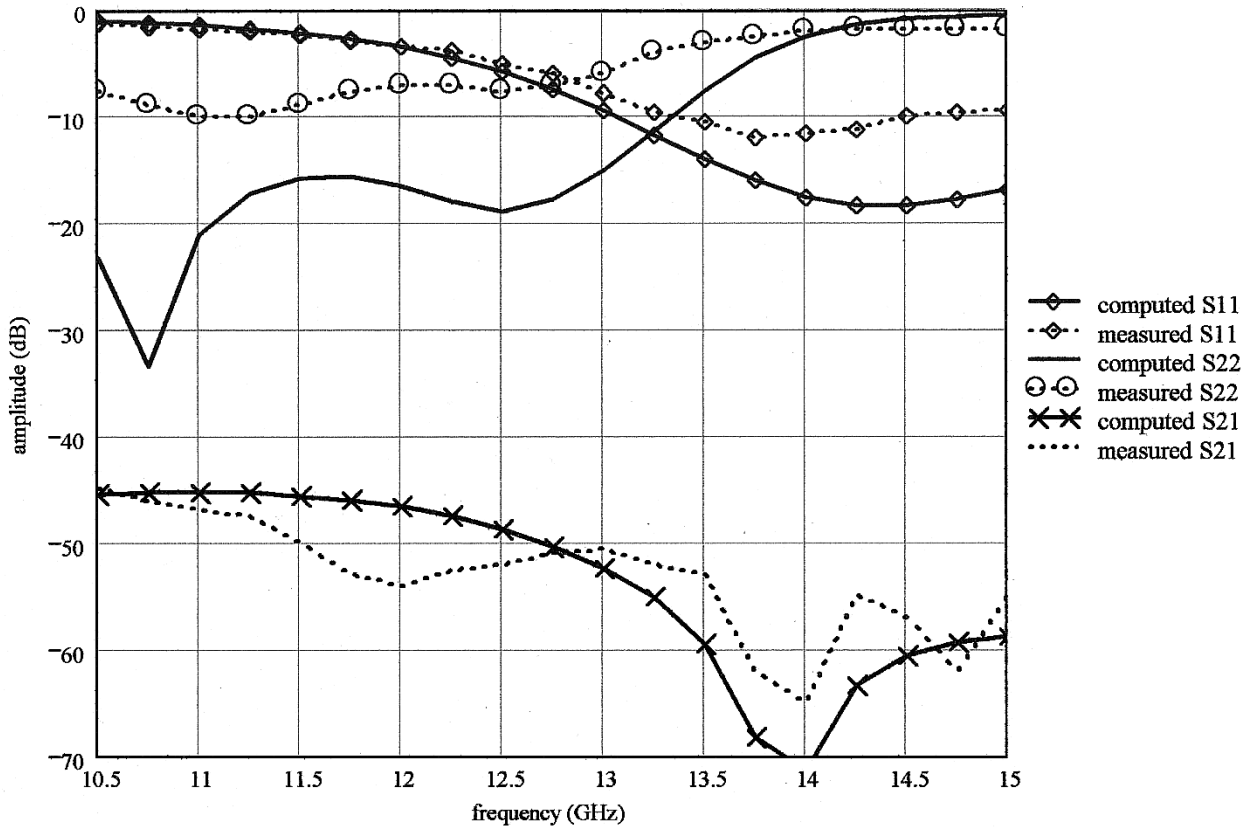

Fig. 12. Computed and measured results of the return loss (S_{11} and S_{22}) and the isolation (S_{21}) between the two ports.

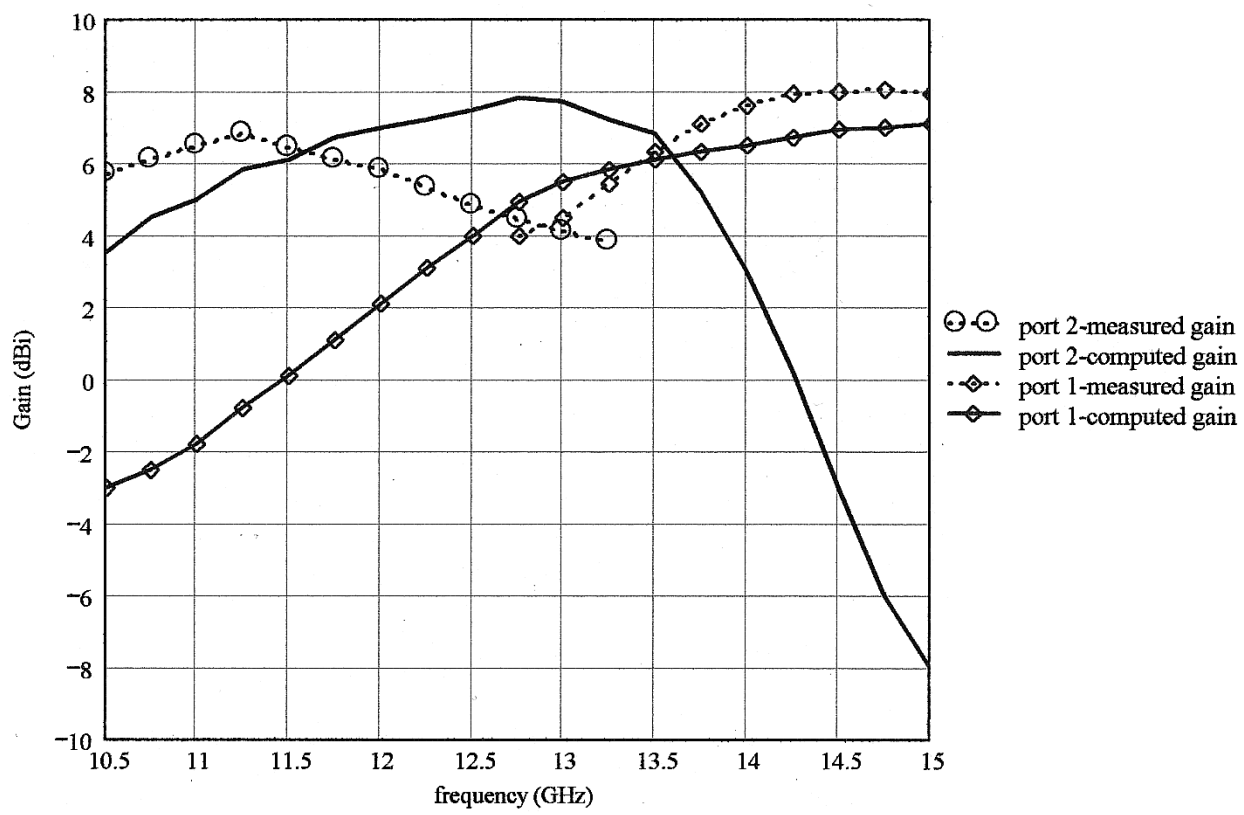

Fig. 13. Computed and measured gain at the two ports of the element.

IV. Conclusion

A new type of a dual-frequency and dual-linear polarization multilayer stacked microstrip antenna element was presented. The microstrip element exhibits a wide band of operation, high isolation between ports, and high radiation efficiency for both polarizations compared to other types of elements. A parametric study was conducted using a commercial software based on MoM algorithm. A prototype with dimensions based on the simulations was built and tested. Conductive vias were used in the stripline feeding structure to suppress the parasitic parallel plate mode. However, the test results show that there is still place for improvement. The agreement between the measured and numerical results is fairly good.

Acknowledgment

The authors wish to thank Dr. G. Kaplan and M. Horev, Gilat Satellite Networks Ltd., for their continued support throughout all phases of this project.

References

[1] F. Croq and D. M. Pozar, "Millimeter-wave design of wide-band aperture-coupled stacked microstrip antennas," *IEEE Trans. Antennas Propagat.*, vol. 12, pp. 1770–1776, Dec. 1991.

[2] S. D. Targonski, R. B. Waterhouse, and D. M. Pozar, "Design of wide-band aperture-stacked patch microstrip antennas," *IEEE Trans. Antennas Propagat.*, vol. 9, pp. 1245–1251, Sept. 1998.

[3] P. B. Katehi, N. G. Alexopoulos, and I. Y. Hsia, "A bandwidth enhancement method for microstrip antennas," *IEEE Trans. Antennas Propagat.*, vol. AP-1, pp. 5–12, Jan. 1987.

[4] D. H. Schaubert and F. G. Farrar, "Some conformal printed circuit antenna designs," in *Proc. Workshop of Printed Technology*, New Mexico State Univ., Las Cruces, NM, 1979, pp. 5.1–5.21.

[5] A. Derneryd, "A theoretical investigation of the rectangular microstrip antenna element," *IEEE Trans. Antennas Propagat.*, vol. AP-7, pp. 532–535, July 1978.

[6] J. Q. Howell, "Microstrip antennas," *IEEE Trans. Antennas Propagat.*, vol. AP-1, pp. 90–93, Jan. 1975.

[7] D. M. Pozar, "A microstrip antenna aperture coupled to a microstripline," *Electron. Lett.*, vol. 21, pp. 49–50, 1985.

[8] C. Chen, W. E. McKinzie III, and N. G. Alexopoulos, "Stripline-fed arbitrarily shaped printed-aperture antennas," *IEEE Trans. Antennas Propagat.*, vol. 7, pp. 1186–1198, July 1997.

[9] P. B. Katehi and N. G. Alexopoulos, "On the modeling of electromagnetically coupled microstrip antennas—the printed strip dipole," *IEEE Trans. Antennas Propagat.*, vol. AP-11, pp. 1179–1186, Nov. 1984.

[10] M. Yamamoto and K. Itoh, "Behavior of parallel plate mode in a slot-coupled patch antenna with stripline feed," in *IEEE Antennas Propagat. Symp. Dig.*, 1998, pp. 932–934.

[11] A. Sabban, "A new broadband stacked two-layer microstrip antenna," *IEEE Antennas Propagat. Symp. Dig.*, pp. 63–66, 1983.

Reuven Shavit (M'82–SM'90) was born in Bucharest, Romania, on November 14, 1949. He received the B.Sc. and M.Sc. degrees in electrical engineering from The Technion, Haifa, Israel, in 1971 and 1977, respectively, and the Ph.D. degree in electrical engineering from the University of California at Los Angeles in 1982.

From 1971 to 1993, he was a Staff Engineer and Antenna Group Leader in the Electronic Research Laboratories of the Israeli Ministry of Defense, Tel Aviv, where he was involved in the design of reflector, microstrip, and slot antenna arrays. He was also a part-time Lecturer at Tel Aviv University, teaching various antenna and electromagnetic courses. From 1988 to 1990, he was associated with ESSCO, Concord, MA, as a Principal Engineer involved in scattering analysis and tuning techniques of high-performance ground-based radomes. Currently, he is a Senior Lecturer with Ben-Gurion University of the Negev, Beer Sheva, Israel, researching microwave components and antennas. His present research interests are in the areas of tuning techniques for radomes and numerical methods for design microstrip, slot, and reflector antennas.

Yuval Tzur was born in Haifa, Israel, on September 21, 1971. He received the B.Sc. degree in electrical and computer engineering from the Ben-Gurion University of the Negev, Beer Sheva, Israel, in 2000.

In 2000, he joined Gilat Satellite Networks, Petah Tikva, Israel, as an Antenna Design Engineer. His main R&D activity was the design of microstrip, dual-band, dual-polarization antennae in the Ku-band for commercial satellite communication use. In May 2001, he joined M.T.I Wireless Edge, Rosh Ha'ayin, Israel, as an Antenna Design Engineer, where he designed dual- and single-polarization CPE antennas, sector antennas, and Omni-directional antennas for the fixed wireless communication market. He also designed Omni-directional antennas for military DF systems, and was involved in the design of reflector antennas for point-to-point applications.

Danny Spirtus (S'97–A'98) was born in Jerusalem, Israel, on April 4, 1969. He received the B.Sc degree in electrical engineering from the Ben-Gurion University, Beer Sheva, Israel, in 1997.

He joined Gilat Satellite Networks, Petah Tikva, Israel, in 1994 and currently serves as the Head of the Antenna and Earth Stations group. His main interests are in the area of microwave antennas and feeds for satellite communication.